

A simulation of asymmetrical voids evolution induced by electromigration

Y.X. Gao, H. Fan ^{*}, Z. Xiao

School of Mechanical and Production Engineering, Nanyang Technological University, Nanyang Avenue, 639798 Singapore, Singapore

Received 11 May 1999; received in revised form 10 January 2000

Abstract

The electromigration-induced asymmetrical evolution of voids in an infinite two-dimensional space is simulated in the present paper. Following a brief review of the general problems and a summary of the fundamental governing equations, we establish a set of the non-linear ODEs with generalized coordinates to describe the evolution of a void with the initial shape bounded by an arbitrary simple closed curve. The present numerical simulation is focused on the features about an elliptical void and the shape asymmetry with respect to the direction of the remote electric field. Two benchmark examples are performed to check our program and several new numerical results are reported to enrich the knowledge on the evolution processes of voids. It is observed that the solution for this problem is sensitive to initial shapes of voids due to its non-linear characteristics. © 2000 Elsevier Science Ltd. All rights reserved.

Keywords: Electromigration; Void evolution; Conformal mapping; Galerkin method; Asymmetry; Numerical simulation

1. Introduction

Materials in their service are seldom in equilibrium state: they evolve. The evolution may affect little on bulk properties of a material, while it changes the microstructures such as microvoids in the material a great deal. Therefore, it is essential to be able to understand microvoids evolution so that the material failure mechanism can be comprehended and controlled to achieve a desired specific engineering requirement. For microdevices whose sizes are in the scale of micro- or nanometers, the evolution is crucial for their performance. Transgranular slit in aluminum interconnects (Suo

et al., 1994) is an example where the microvoid evolution has found its useful application in chip industry. The evolution phenomena in the micro-electronic devices are of great importance to the academic research as well as the microelectronic industry.

One of the evolution phenomena is electromigration-induced void evolution. Experimental evidence (Sanchez et al., 1992; Rose, 1992) showed that an aluminum interconnect often fails by a transgranular slit. The sequence of the events has also been revealed that a round void nucleates first, enlarging and drifting, and then collapses to a narrow slit (Kraft et al., 1993; Arzt et al., 1994). Suo et al. (1994) showed how electric current causes the void shape instability. The summarization of the existing analytical solution of a translating circular void was given by Wang et al. (1996). They showed that a circular void translating in

^{*} Corresponding author. Tel.: +65-790-4860; fax: +65-791-1859.

E-mail address: mhfan@ntu.edu.sg (H. Fan).

an infinite, isotropic conductor is stable against any infinitesimal shape perturbation. On the other hand, a finite shape imperfection may lead to a slit. Indeed, recent simulations showed that a circular void in an interconnect of finite width is unstable and evolves to a slit (Kraft and Arzt, 1995; Xia et al., 1997).

More recent works are very helpful for understanding the electromigration phenomena. Schimschak and Krug (1997) demonstrated the intriguing phenomenon induced by surface electromigration as a moving boundary value problem. In a follow-up paper (Schimschak and Krug, 1998), they simulated the electromigration-induced break-up of two-dimensional voids. Simulations and theory of slit formation induced by electromigration in unpassivated single-crystal metal lines were presented by Mahadevan and Bradley (1999). They considered the competition among surface electromigration, surface self-diffusion and current crowding. Wang et al. (1996) simulated an insulating void in an infinite conductor, and introduced finite imperfection to the initial void shape. They showed that the void evolution and its stability depended on not only the electric field intensity, but also the type and magnitude of the initial shape imperfection. In their simulation, the initial void shape and the shape at any time during the void evolution were assumed to be mirror symmetry with respect to the direction of the remote electric field submitted to the conductor. It is noticed that the asymmetrical cases have not been reported in the literature. Therefore, it is the objective to investigate the shape asymmetry and evolution process.

In the following sections, the electromigration-induced evolution of an arbitrary shape void in an infinite two-dimensional space is studied via a thermodynamic consideration (Suo, 1997; Yang and Suo, 1996). Based on their theory, our attention is focused on the shape asymmetry with respect to the direction of the remote field. The solution of the electric field around a void with arbitrary shape in an infinite conductor is outlined and the system of the non-linear ODEs with generalized coordinates to describe the evolution of a void is established in Section 3. In Section 4, we have performed several case studies to check our

numerical program and to illustrate the phenomena of various evolution processes. Conclusion and discussion are given in Section 5.

2. Governing equations

The fundamental laws governing the evolution phenomenon of a microvoid in an interconnect subjected to an electric field are briefly discussed in the present section. Meanwhile, the assumptions made in this paper are also outlined. For further details about the general formulation of motions of microscopic surface in materials, one may refer to Suo (1997).

2.1. Kinematics equations

Fig. 1 illustrates an insulating void with arbitrary shape in an interconnect under a remote uniform electric field E . To avoid the mathematical formidableness, we examine a two-dimensional problem of a cylindrical void in an interconnect. It has been assumed that the interconnect is infinite one because the scale of the void is very small as compared with the scale of the interconnect. The void shifts its location and changes its shape by mass diffusion on the void surface. It is obvious that the mathematical problem corresponding to the physical phenomenon of voids evolution mentioned above is to evolve a closed curve in a two-dimensional plane.

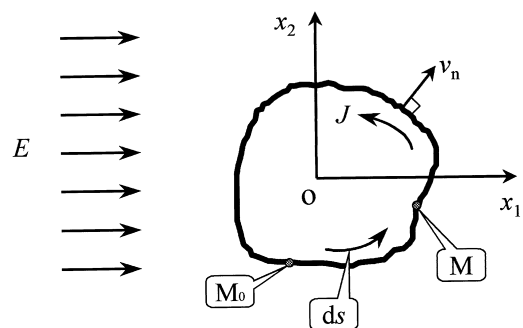


Fig. 1. An arbitrary shape void in an interconnect subjected to a uniform electric field.

Let us describe the closed curve at a given time t by the position vector \mathbf{x} as the function of a parameter θ , namely,

$$\mathbf{x} = \mathbf{x}(\theta, t). \quad (2.1)$$

At an arbitrary time, the length of an arc element ds , the unit vector normal to the arc element \mathbf{n} , and the curvature of the arc element κ can be derived from (2.1). A sign convention is adopted that \mathbf{n} points from the void to the solid, and $\kappa > 0$ for a circular void. Denote the velocity normal to the surface of the void by v_n (i.e., the volume of mass removed from unit surface area in unit time). It relates to the position vector as

$$v_n = \mathbf{n} \cdot \frac{\partial \mathbf{x}}{\partial t} = \frac{\partial x_2}{\partial s} \frac{\partial x_1}{\partial t} - \frac{\partial x_1}{\partial s} \frac{\partial x_2}{\partial t}, \quad (2.2)$$

where s in Eq. (2.2) stand for the arc length measured from a convenient point on the void surface.

Let J be the atomic flux on the void surface (i.e., the number of atoms crossing unit arc length on the surface in unit time). Mass conservation (Suo, 1997) requires that the velocity normal to the void surface relates to the flux divergence as

$$v_n = \Omega \frac{\partial J}{\partial s}, \quad (2.3)$$

where Ω is the volume per atom. Eqs. (2.1)–(2.3) describe the kinematics of the dynamic system of a void evolution in the two-dimensional plane.

2.2. Electron wind force and electric field

The electron wind exerts a force, F_E , on an atom on the void surface in the direction of the electron flow with the magnitude proportional to the electric field (Yang and Suo, 1996; Suo, 1997). Let E_T be the component of the electric field tangential to the void surface. The electron wind force per atom is written as

$$F_E = -Z^* e E_T, \quad (2.4)$$

where Z^* (>0) is the effective valence, and e (>0) is the magnitude of the electron charge. The subscripts E and T on F_E and E_T stand for the electron wind force and the tangential component of electric field, respectively. The negative sign in Eq.

(2.4) means that the force is in the direction of the electron flow.

To determine the electron wind force, it is required that the electric field can be solved for the given void shape at an arbitrary time. We assume that the electric field distribution obeys the standard equations summarized below. The electric field vector E is the gradient of the electric potential ϕ , namely,

$$E_i = -\Phi_{,i}. \quad (2.5)$$

The electric current density vector, \mathbf{j} , meets the requirement of electric charge conservation,

$$j_{i,i} = 0. \quad (2.6)$$

The electric field relates to the current density by Ohm's law

$$E_i = \rho j_i, \quad (2.7)$$

where ρ is the resistivity. The resistivity of aluminum is isotropic. A combination of Eqs. (2.5)–(2.7) shows that the electric potential obeys the Laplace equation:

$$\phi_{,ii} = 0. \quad (2.8)$$

This partial differential equation, together with boundary conditions, determines the electric potential. The electric field component tangential to the void perimeter is calculated from the gradient of the electric potential in the direction of the arc length:

$$E_T = -\frac{\partial \phi}{\partial s}. \quad (2.9)$$

An aluminum interconnect is typically subject to an electric field below 1000 V/m. This electric field is amplified at the void. For a void without sharp edges, the amplification factor is about 2. Since the electric field inside the void is much lower than the electrical breakdown field of vacuum or dry air (around 1 MV/m), the void can be modeled as an insulator, namely, $\mathbf{j} \cdot \mathbf{n} = 0$ on the void surface.

2.3. Diffusion driving force and weak statement

Generally, G , the free energy of the system, consists of surface energy and electrostatic energy. Both of them vary when the void changes its

shape. Nevertheless, the electrostatic energy is much smaller than the surface energy for our cases. Therefore, the electrostatic energy will be ignored in the following formulae. The free energy only takes the surface energy as

$$G = \int \gamma \, ds. \quad (2.10)$$

The integral extends over the void surface. The surface tension γ may depend on crystal orientation, but it is assumed to be an isotropic material constant in this study.

Next, the driving force contributed by mass diffusion has been defined by using virtual motion. Let δI be the virtual mass displacement (i.e., the number of atoms across unit length on the surface). Associated with this virtual motion, the free energy changes by δG , and the electron wind force does work, $\int F_E \delta I \, ds$. The diffusion driving force, F , is then defined by

$$\int F \delta I \, ds = -\delta G + \int F_E \delta I \, ds. \quad (2.11)$$

In other words, F is the reduction in the free energy plus the work done by the electron wind force, with respect to one atom moving unit distance on the surface.

Mass conservation relates the small virtual migration normal to surface, δr_n , to the virtual mass displacement δI as

$$\delta r_n = \Omega \frac{\partial(\delta I)}{\partial s}. \quad (2.12)$$

It is similar to the relationship between the surface velocity, v_n , and the atomic flux, J in Eq. (2.3). Actually, both (2.3) and (2.12) embody the fundamental law of mass conservation.

The linear kinetic law is adopted as

$$J = MF. \quad (2.13)$$

It connects the flux with the total diffusion driving force linearly. This equation defines the atomic mobility on the interface, M . Frequently, the atomic mobility is a second-order tensor at any one point on the interface, and may also vary from point to point. In current research, we assume that the mobility is independent of the crystalline di-

rection, namely, it is isotropic. The mobility is generally determined in practice either by observing a phenomenon or by an atomistic simulation. The mobility relates to the self-diffusivity by the Einstein relation, $M = D\delta/\Omega kT$, where D is the self-diffusivity on the interface, δ the effective thickness of atoms that participate in mass transport, k Boltzmann's constant, and T is the absolute temperature.

By substituting (2.13) into (2.11), a so-called "weak statement" of the dynamic system is obtained as

$$\int \frac{J}{M} \delta I \, ds = -\delta G + \int F_E \delta I \, ds. \quad (2.14)$$

The actual flux J satisfies (2.14) for arbitrary virtual motion δI . In other words, the actual flux, of all virtual flux J^* , minimizes the functional

$$\Pi = \frac{\partial G}{\partial t} - \int F_E J^* \, ds + \int \frac{J^{*2}}{2M} \, ds. \quad (2.15)$$

Eq. (2.14) is the global governing equation of the evolution system. It determines the actual evolution path of a void, and therefore its location and shape.

3. The evolution of generalized coordinates

3.1. The complex variables description of the void shape and location

The void shape characterized by a closed curve can be described by (2.1), the position vector \mathbf{x} as the function of a parameter θ at a given time t . Equivalently, it can also be described by the complex function $z = z(\theta)$ in z -plane at a given time t , where complex variable $z = x_1 + ix_2$ and $i = \sqrt{-1}$. Following the conformal mapping method, let S be an infinite external region of the void bounded by one arbitrary simple closed curve L . The region S be mapped on to the exterior of the unit circle illustrated in Fig. 2, $\zeta = \exp(i\theta)$ ($0 \leq \theta < 2\pi$), of the ζ -plane by the function expanded in a series of the form

$$z = a_{-1}\zeta + a_0 + \sum_{n=1}^{\infty} a_n \zeta^{-n}, \quad (3.1)$$

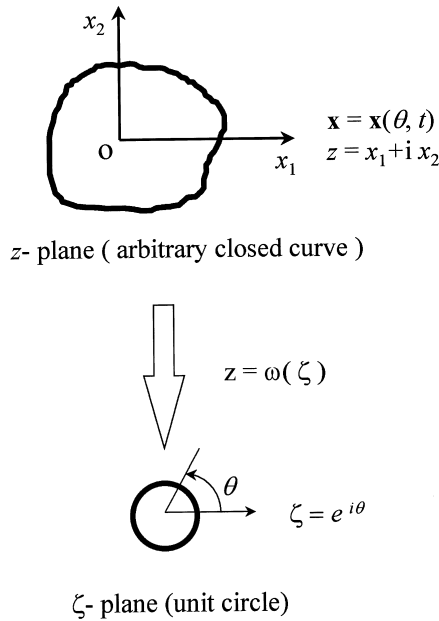


Fig. 2. The map between the void in the z -plane and the unit circle in the ζ -plane.

where all of the coefficients $\{a_{-1}, a_0, a_1, a_2, \dots, a_n, \dots\}$ are complex numbers. If one only retains the first m terms of (3.1), then

$$z = a_{-1}\zeta + a_0 + \sum_{n=1}^m a_n \zeta^{-n} \tag{3.2}$$

will map on to the unit circle the region S_m , and not S . If one takes m sufficiently large, the region S_m will be as close as one pleases to the region S . Thus, one may practically solve a given problem for the region S_m by retaining a number of terms in (3.1) which will be sufficient for the stated purpose, and the solution will represent an approximate solution for the original region S .

If one writes the coefficients $\{a_k\}$ ($k = -1, 0, 1, 2, \dots, m$) in real numbers as

$$a_k = r_k \exp(i\varphi_k) \quad (k = -1, 0, 1, 2, \dots, m), \tag{3.3}$$

where all the coefficients r_k and φ_k are real numbers, one has the following real number expansions instead of (3.2):

$$x_1 = r_{-1} \cos(\varphi_{-1} + \theta) + r_0 \cos \varphi_0 + \sum_{n=1}^m r_n \cos(\varphi_n - n\theta), \tag{3.4a}$$

$$x_2 = r_{-1} \sin(\varphi_{-1} + \theta) + r_0 \sin \varphi_0 + \sum_{n=1}^m r_n \sin(\varphi_n - n\theta). \tag{3.4b}$$

According to (3.4a) and (3.4b), a point on the unit circle at angle θ on ζ -plane maps onto a point on the void perimeter, (x_1, x_2) , on the z -plane.

It is noted that the parametric equations (3.4a) and (3.4b) describe an arbitrary closed curve L in the z -plane and the parameter in (3.4a) and (3.4b) is just the complex angle θ on the ζ -plane. Moreover, the shape and location of the closed curve L in the z -plane, which represents the shape and location of the void in an interconnect at a given time, are characterized by the coefficients $\{r_{-1}, r_0, r_1, \dots, r_m; \varphi_{-1}, \varphi_0, \varphi_1, \dots, \varphi_m\}$ in the parametric equations (3.4a) and (3.4b). For convenience, these coefficients will be denoted by $\{r_k; \varphi_k\}$ ($k = -1, 0, 1, \dots, m$). Meanwhile, it is also noted that the coefficients $\{r_k; \varphi_k\}$ evolve with time when the void evolves with time. But the unit circle on the ζ -plane remains unchanged at any time.

In the present study, the coefficients $\{r_k; \varphi_k\}$ are chosen as the generalized coordinates of the system of void evolution to describe the changes of the shape and location of the void. The generalized velocities are written as $\{\dot{r}_k; \dot{\varphi}_k\}$, and the d.f., d , of the system of generalized coordinates is $2(m + 2)$. The following numerical results are computed with the d.f. $d = 20$.

3.2. Electric field around an arbitrary shape void in an infinite conductor

In order to determine the electron wind force on the atom on the void surface at any time, it is essential to solve the electric field around an arbitrary shape void in an infinite plane under a remote uniform electric field. Since the electric potential ϕ is a harmonic function, the solution can be readily obtained by complex function methods. Let $\omega(z)$ be an arbitrary holomorphic function of complex variable z in the region S of the z -plane. The general solution of a harmonic function is

$$\phi = \text{Re}[\omega(z)], \tag{3.5}$$

where “Re” denotes “the real part” of a complex function and “Im” will denote “the imaginary part” in the following. The electric current density flowing across an arbitrary segment M_0M which connects arbitrarily fixed point M_0 with the variable point M and which does not leave the region S (Fig. 1), is determined by the formula

$$\int_{M_0M} \mathbf{j} \cdot \mathbf{n} \, ds = -\frac{1}{\rho} \operatorname{Im}[\omega(z)]. \tag{3.6}$$

To determine the holomorphic function $\omega(z)$, it is necessary to state the boundary conditions. As we know, the electric field is E when $|z| \rightarrow \infty$, and the electric current density normal to the void surface is equal to zero, namely, $\mathbf{j} \cdot \mathbf{n} = 0$. With the help of Eqs. (2.5) and (3.6), the boundary condition can be written as

$$\omega(z) \rightarrow -Ez \quad \text{when } |z| \rightarrow \infty, \tag{3.7a}$$

$$\operatorname{Im}[\omega(z)] = 0 \quad \text{on the void surface.} \tag{3.7b}$$

By contrast with the closed-form solution for a circular void within an infinite plane, considering the boundary conditions (3.7a) and (3.7b), the form of $\omega(z)$ on the void surface in the ζ -plane is obtained:

$$\omega = -a_{-1}E(\zeta + \zeta^{-1}). \tag{3.8}$$

The implicit-function form of $\omega(z)$ in the z -plane is determined by Eqs. (3.2) and (3.8). The electric potential on the void surface is determined by (3.5) as

$$\phi = -2Er_{-1} \cos \varphi_{-1} \cos \theta. \tag{3.9}$$

This solution is valid for the insulating void described by the parametric equations (3.4a) and (3.4b) with generalized coordinates in an infinite two-dimensional space where a remote uniform electric field E is acting in the positive direction of x_1 -axis.

3.3. The evolution of generalized coordinates

We have completed the description for the shape and location of a void at a given time by generalized coordinates in the last subsections. The

evolution of generalized coordinates characterizes the void evolution with the time. In this subsection, we consider the equations governing the evolution of generalized coordinates in process of the void evolution with the time.

Substituting (2.2) into (2.3) gives

$$\Omega \frac{\partial J}{\partial s} = \frac{\partial x_2}{\partial s} \frac{\partial x_1}{\partial t} - \frac{\partial x_1}{\partial s} \frac{\partial x_2}{\partial t}. \tag{3.10}$$

Equivalently, it can be written as

$$\Omega \frac{\partial J}{\partial \theta} = \frac{\partial x_2}{\partial \theta} \frac{\partial x_1}{\partial t} - \frac{\partial x_1}{\partial \theta} \frac{\partial x_2}{\partial t} \tag{3.11}$$

with the differential relationship between the two arguments s and θ :

$$ds = \sqrt{(dx_1)^2 + (dx_2)^2} = S(\theta) \, d\theta, \tag{3.12a}$$

where

$$S(\theta) = \sqrt{\left(\frac{\partial x_1}{\partial \theta}\right)^2 + \left(\frac{\partial x_2}{\partial \theta}\right)^2}. \tag{3.12b}$$

Consequently, we have

$$J(\theta) = \frac{1}{\Omega} \int_0^\theta \left(\frac{\partial x_2}{\partial \theta} \frac{\partial x_1}{\partial t} - \frac{\partial x_1}{\partial \theta} \frac{\partial x_2}{\partial t} \right) \, d\theta \tag{3.13}$$

subject to taking $s = 0$ at $\theta = 0$ and $J = 0$ at $\theta = 0$.

Substituting parametric equations (3.4a) and (3.4b) into (3.13) and integrating the right-hand side of (3.13) gives

$$\Omega J(\theta) = \sum_k A_k \dot{r}_k + \sum_k B_k \dot{\varphi}_k \quad (k = -1, 0, 1, \dots, m) \tag{3.14}$$

with

$$A_{-1} = r_{-1}\theta + \sum_{n=1}^m \frac{n}{n+1} r_n \{ \sin[\varphi_n - \varphi_{-1}] - (n+1)\theta \} - \sin[\varphi_n - \varphi_{-1}], \tag{3.15a}$$

$$A_0 = -r_{-1}[\sin(\varphi_0 - \varphi_{-1} - \theta) - \sin(\varphi_0 - \varphi_{-1})] + \sum_{n=1}^m r_n [\sin(\varphi_n - \varphi_0 - n\theta) - \sin(\varphi_n - \varphi_0)], \tag{3.15b}$$

$$\begin{aligned}
 A_k = & -r_{-1} \frac{1}{k+1} \{ \sin[\varphi_k - \varphi_{-1} - (k+1)\theta] \\
 & - \sin(\varphi_k - \varphi_{-1}) \} \\
 & + \sum_{\substack{n=1 \\ n \neq k}}^m \frac{n}{n-k} r_n \{ \sin[\varphi_n - \varphi_k - (n-k)\theta] \\
 & - \sin(\varphi_n - \varphi_k) \} - kr_k \theta, \quad (3.15c)
 \end{aligned}$$

$$\begin{aligned}
 B_{-1} = & -r_{-1} \sum_{n=1}^m \frac{n}{n+1} r_n \{ \cos[\varphi_n - \varphi_{-1} \\
 & - (n+1)\theta] - \cos[\varphi_n - \varphi_{-1}] \}, \quad (3.15d)
 \end{aligned}$$

$$\begin{aligned}
 B_0 = & -r_0 r_{-1} [\cos(\varphi_0 - \varphi_{-1} - \theta) - \cos(\varphi_0 - \varphi_{-1})] \\
 & - \sum_{n=1}^m r_0 r_n [\cos(\varphi_n - \varphi_0 - n\theta) - \cos(\varphi_n - \varphi_0)], \quad (3.15e)
 \end{aligned}$$

$$\begin{aligned}
 B_k = & -r_k r_{-1} \frac{1}{k+1} \{ \cos[\varphi_k - \varphi_{-1} - (k+1)\theta] \\
 & - \cos(\varphi_k - \varphi_{-1}) \} - r_k \sum_{\substack{n=1 \\ n \neq k}}^m \frac{n}{n-k} r_n \\
 & \times \{ \cos[\varphi_n - \varphi_k - (n-k)\theta] - \cos(\varphi_n - \varphi_k) \}, \quad (3.15f)
 \end{aligned}$$

where the subscripts k on the formulas of A_k and B_k can be evaluated as $k = 1, 2, \dots, m$.

Eq. (3.14) shows that the flux J is linear with the generalized velocities $\{\dot{r}_k; \dot{\varphi}_k\}$, so that it satisfies the kinematics requirement. The fact that the flux $J(\theta)$ is a periodic function with the period of 2π , namely, $J(\theta) = J(\theta + 2\pi)$, gives a constrained condition

$$r_{-1} \dot{r}_{-1} - \sum_{k=1}^m k r_k \dot{r}_k = 0. \quad (3.16)$$

The condition (3.16) means that the area of the void remains unchanged when the shape and location of the void change with the time. It fulfills the requirement of mass conservation. The combination of (3.14), (3.15a)–(3.15f) and (3.16) shows that the aperiodic terms, $r_{-1}\theta$ and $kr_k\theta$, must vanish in Eqs. (3.15a)–(3.15f). The constrained

condition (3.16) will be fulfilled in the following numerical procedure.

For the sake of convenience, the equations will be written in dimensionless form. All the variables that have length dimension are normalized by a selected initial length R_0 which measures the initial scale of the void. For example, let R_0 be the initial radius as the initial shape of the void is a circle and R_0 be the average radius, $(a_0 + b_0)/2$, as the initial shape of the void is an ellipse, where a_0 and b_0 denote the major semi-axis and minor semi-axis of the ellipse, respectively. Meanwhile, all the variables that have the same dimension as the electric field are normalized by the remote electric field E . Consequently, the dimensionless generalized coordinates are denoted as

$$\begin{aligned}
 \{q_i\} = & \{r_{-1}/R_0, r_0/R_0, r_1/R_0, \dots, r_m/R_0, \varphi_{-1}, \\
 & \varphi_0, \varphi_1, \dots, \varphi_m\}, \quad (3.17)
 \end{aligned}$$

where subscripts $i = 1, 2, \dots, 2(m+2)$, and the dimensionless generalized velocities are written as $\{\dot{q}_i\}$. Thus, the flux (3.14) is written as

$$J(\theta) = \frac{R_0^2}{\Omega} \sum_{i=1}^{2(m+2)} N_i \dot{q}_i \quad (3.18)$$

with

$$\begin{aligned}
 \{N_i\} = & \left\{ \frac{A_{-1}}{R_0}, \frac{A_0}{R_0}, \frac{A_1}{R_0}, \dots, \frac{A_m}{R_0}, \right. \\
 & \left. \frac{B_{-1}}{R_0^2}, \frac{B_0}{R_0^2}, \frac{B_1}{R_0^2}, \dots, \frac{B_m}{R_0^2} \right\} \quad (3.19)
 \end{aligned}$$

and the virtual mass displacement δI is written as

$$\delta I = \frac{R_0^2}{\Omega} \sum_{i=1}^{2(m+2)} N_i \delta q_i. \quad (3.20)$$

Substituting Eqs. (3.18) and (3.20) into weak statement (2.14), with the help of Eqs. (2.4), (2.9), (2.12) and integrating by parts, we obtain finally

$$\begin{aligned}
 \frac{R_0^2}{M\Omega^2} \sum_{i,j=1}^{2(m+2)} N_i N_j \, ds \, \dot{q}_i \delta q_j = & \gamma \sum_{j=1}^{2(m+2)} \int \frac{\partial \kappa}{\partial s} N_j \, ds \, \delta q_j \\
 & + \frac{Z^* e}{\Omega} \sum_{j=1}^{2(m+2)} \int \frac{\partial \phi}{\partial s} N_j \, ds \, \delta q_j, \quad (3.21)
 \end{aligned}$$

where the integrals extend over the whole perimeter of the void. Bear in mind that Eq. (3.21) must hold true for any virtual motion δq_j , so that

$$\frac{R_0^2}{M\Omega^2} \sum_{i=1}^{2(m+2)} \int N_i N_j \, ds \, \dot{q}_i = \gamma \int \frac{\partial \kappa}{\partial s} N_j \, ds + \frac{Z^* e}{\Omega} \int \frac{\partial \phi}{\partial s} N_j \, ds \quad (3.22)$$

with $j = 1, 2, \dots, 2(m+2)$. By introducing a dimensionless group χ and a characteristic time t_0 (Suo, 1997) as

$$\chi = \frac{Z^* e E R_0^2}{\Omega \gamma}, \quad t_0 = \frac{R_0^4}{M \Omega^2 \gamma}, \quad (3.23)$$

one writes Eq. (3.22) in a dimensionless form as

$$\sum_{i=1}^{2(m+2)} H_{ij} \frac{dq_i}{dt} = f_j^S + \chi f_j^E, \quad j = 1, 2, \dots, 2(m+2) \quad (3.24)$$

with

$$H_{ij} = \int N_i N_j \, ds, \quad f_j^S = \int \frac{\partial \kappa}{\partial s} N_j \, ds, \quad f_j^E = \int \frac{\partial \phi}{\partial s} N_j \, ds. \quad (3.25)$$

All the variables in Eq. (3.24) denote their dimensionless forms. For example, the dimensionless time t in (3.24) means t/t_0 , but is still denoted as t for convenience. From Eqs. (3.24) and (3.25), it is noted that the energetic driving force for void evolution, conjugating to the generalized coordinates, consists of two parts, f_j^S and f_j^E , resulting from the surface tension and the electron wind, respectively. The system of equations (3.24) furnishes a dynamic system with the generalized coordinates $\{q_i\}$ to govern the evolution of the generalized coordinates so as to govern the void evolution. The process of voids evolution depends on the solution of the system of Eqs. (3.24) under

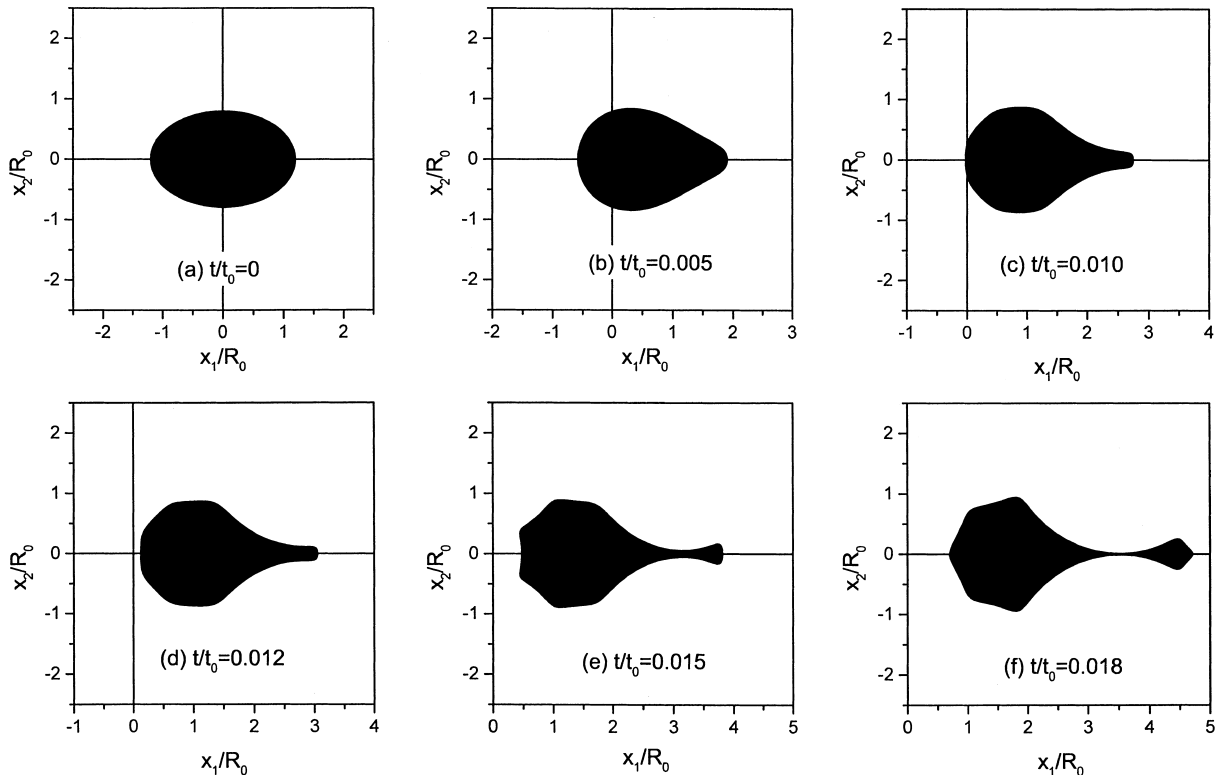


Fig. 3. The traces of the void shape at stated times ($\chi = 47, m_0 = 0.2, \beta_0 = 0$).

the external control parameters $\{\chi, t_0\}$ and the initial-value condition

$$q_i(t)|_{t=0} = q_i(0), \quad i = 1, 2, \dots, 2(m + 2), \quad (3.26)$$

where the initial values $\{q_i(0)\}$ describe the initial shape and location of the void. In other words, the system of the first-order non-linear equations (3.24) with the initial-value conditions (3.26) governs the void evolution.

4. Numerical simulation

It is the purpose in this section to give numerical simulations for the solutions of the system (3.24). As an example, let us simulate the electromigration-induced evolution of an elliptical void in an infinite two-dimensional space. Considering an ellipse with initial shape and location given by

$$x_1 = R_0[\cos(\beta_0 + \theta) + m_0 \cos(\beta_0 - \theta)], \quad (4.1a)$$

$$x_2 = R_0[\sin(\beta_0 + \theta) + m_0 \sin(\beta_0 - \theta)] \quad (4.1b)$$

with

$$R_0 = \frac{a_0 + b_0}{2}, \quad m_0 = \frac{a_0 - b_0}{a_0 + b_0}, \quad (4.2)$$

where a_0 and b_0 are the two semi-axes of the ellipse, and β_0 is the angle measured from the axis x_1 to the semi-axis a_0 of the ellipse in the anti-clockwise direction. We call β_0 the orientation angle, R_0 the average radius and m_0 the degree of an ellipse, respectively. It is clear that the initial shape of an elliptical void depends on three parameters: R_0 , m_0 and β_0 . Making a comparison between Eqs. (3.4a) and (3.4b) and (4.1a) and (4.1b) gives that the initial-value conditions (3.26) for an elliptical void are written as

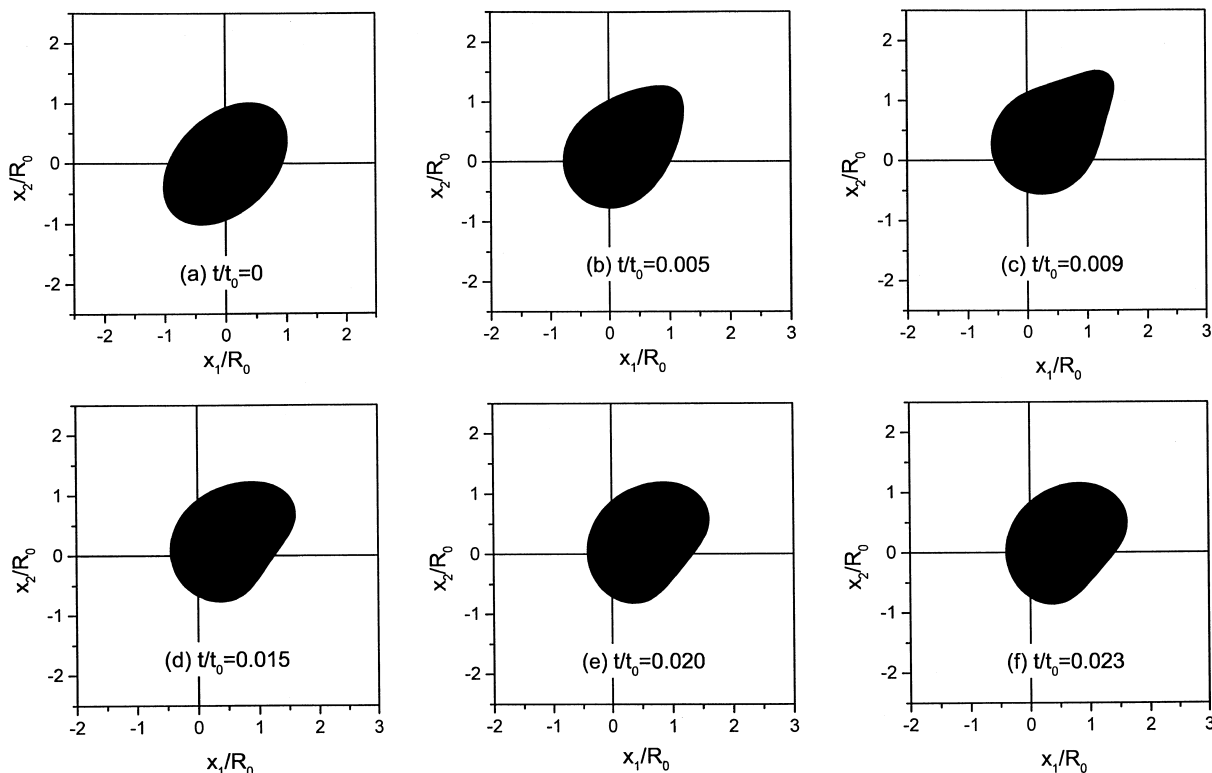


Fig. 4. The traces of the void shape at stated times ($\chi = 47$, $m_0 = 0.2$, $\beta_0 = \pi/4$).

$$\begin{aligned}
 q_1(0) &= 1, & q_3(0) &= m_0, & q_{m+3}(0) &= \beta_0, \\
 q_{m+5}(0) &= \beta_0, & q_i(0) &= 0 & \text{for other } i.
 \end{aligned}
 \tag{4.3}$$

Consequently, the electromigration-induced evolution of an elliptical void in an infinite interconnect is governed by the set of non-linear ODEs (3.24) with the constrained condition (3.16) and the initial-value condition (4.3). Therefore, the evolution process of the elliptical void depends on the external control parameters χ and t_0 and the initial-value parameters m_0 and β_0 . Standard numerical methods are used to calculate the integrals (3.25) and solve the system of equations (3.24) for $q_i(t)$ at various χ , m_0 and β_0 . The Simpson's method is used to evaluate the integrals and the fourth-order Runge-Kutta method to solve the system of ODEs. We have performed

several case studies to check our program and to illustrate the phenomena of various evolution processes.

4.1. Benchmark examples

In order to ensure our numerical scheme, we considered case 1 as follows.

Case 1: $\chi = 0$, $m_0 = 0.7$, $\beta_0 = 0$.

In this case, the void evolution is only driven by the surface tension. The elliptical void changes its shape so as to reduce its surface area and evolve into a circular void finally, but remains its location unchanged. Our simulation gives the expected result, which is the same as the FEM result given by Xia et al. (1997).

As the second test, we considered case 2 as follows.

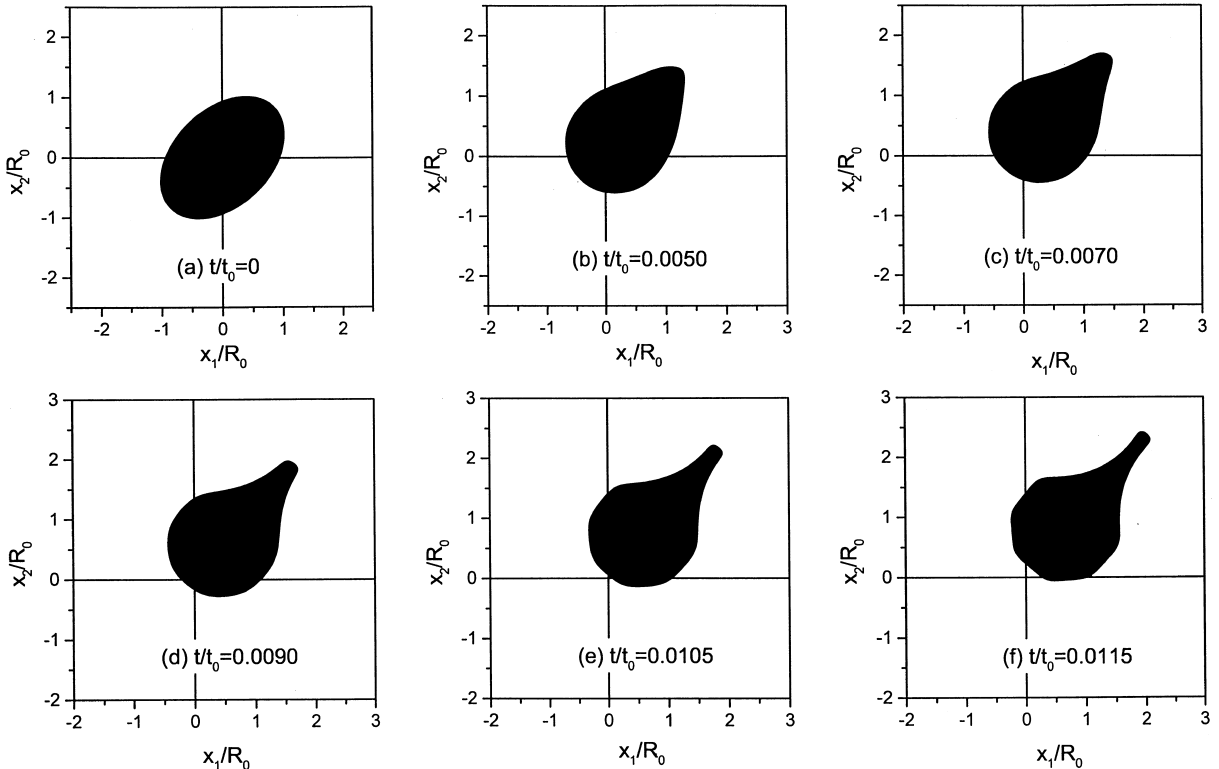


Fig. 5. The traces of the void shape at stated times ($\chi = 80$, $m_0 = 0.2$, $\beta_0 = \pi/4$).

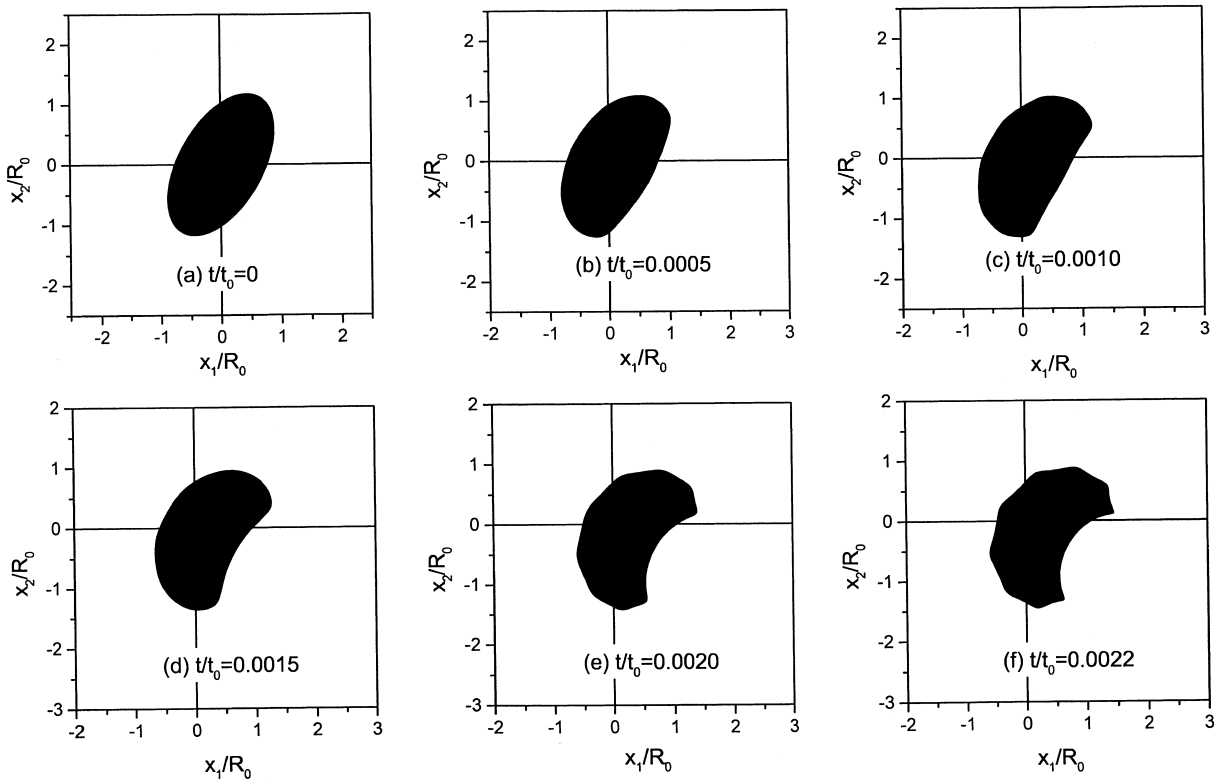


Fig. 6. The traces of the void shape at stated times ($\chi = 100$, $m_0 = 0.3$, $\beta_0 = \pi/3$).

Case 2: $\chi \neq 0$, $m_0 = 0$.

The initial shape of the void is a perfect circle, and β_0 disappears in this case. The exact solution given by Ho (1970) showed that the circular void migrates without changing its shape, in the direction of the remote electric field (the positive direction of x_1 -axis). Its migration speed can be calculated exactly. In this case, our numerical program gives that the circular void migrates in the direction of x_1 -axis and remains the circular shape unchanged. Quantitatively, the migration speed given by our simulation is the same as Ho's solution.

4.2. Electromigration of an elliptical void

To reveal how the evolution of the void depends on the external control parameters χ and t_0 and initial value m_0 and β_0 , we have performed many

case studies. Figs. 3–6 illustrate several selected cases including the following cases.

Case 3: $\chi = 47$, $m_0 = 0.2$, $\beta_0 = 0$.

Case 4: $\chi = 47$, $m_0 = 0.2$, $\beta_0 = \pi/4$.

Case 5: $\chi = 80$, $m_0 = 0.2$, $\beta_0 = \pi/4$.

Case 6: $\chi = 100$, $m_0 = 0.3$, $\beta_0 = \pi/3$.

These figures show the traces of the void shape and locations at stated times.

From Figs. 3–6, it can be seen that the process of a void evolution consists of the shape changing, the location shifting and the orientation rotating of the void. These typical numerical solutions can give us the overview of the evolution process of an elliptical void and its dependence on the parameter χ and the initial value m_0 and β_0 . The comparison between Figs. 3 and 4 shows that the orientation angle β_0 is an important parameter that affects the evolution process and the final state. It should be noted that the curves in Figs. 3(f) and 6(f) are not smooth enough due to limited d.f. in the simulation.

5. Conclusion and discussion

The evolution process of a void with the initial shape bounded by an arbitrary simple closed curve can be modeled by a system of non-linear ODEs with generalized coordinates. The solution for this system is sensitive to the initial values of the void shape due to the non-linear characteristics of the ODEs. Therefore, it is essential to perform large number of numerical simulations with respect to various control parameters and initial-value conditions to reveal the mechanisms of the evolution of voids.

The present numerical study is focused on the void with an elliptical initial shape and the shape asymmetry. The results show that the void is shifting its location, rotating its orientation and changing its shape during the process of evolution. The orientation angle β_0 of the elliptical void is an important parameter that affects the evolution process and the final state. The angle causes the asymmetric features with respect to the direction of the remote electric field, including the initial and changed shape as well as the location change of the void (Figs. 4–6). Various angles cause different shapes during the evolution under the same parameters χ and m_0 (Figs. 3 and 4).

The final shape of a void evolution depends on the solution for the set of ODEs. If the solution is stable, there will be a final shape of the evolution void; otherwise the scenario could be very complicated. From our case studies, the void reaches a stable shape as the parameters χ and m_0 are small, such as the special cases illustrated in Fig. 4; the void may be unstable as the parameters χ and m_0 are large, such as Figs. 5 and 6. Wang et al. (1996) showed that a symmetrical void collapses to a slit when χ is large. Xia et al. (1997) and Schimschak and Krug (1998) indicated that a large void breaks up into two or more smaller cavities. Unfortunately, our numerical simulation cannot give the void shape after the void reaches unstable state. Further researches are needed to reveal the mechanisms.

Acknowledgements

This work is partially funded by National Science and Technology Board of Singapore under University R&D Program.

References

- Arzt, E., Kraft, O., Nix, W.D., Sanchez, J.E., 1994. Electromigration failure by shape change of voids in bamboo lines. *J. Appl. Phys.* 76, 1563–1796.
- Ho, P.S., 1970. Motion of inclusion induced by a direct current and a temperature gradient. *J. Appl. Phys.* 41, 64–68.
- Kraft, O., Arzt, E., 1995. Numerical simulation of electromigration-induced shape changes of voids in bamboo lines. *Appl. Phys. Lett.* 66, 2063–2065.
- Kraft, O., Bader, S., Sanchez, J.E., Arzt, E., 1993. Observation and modeling of electromigration-induced void growth in Al-based interconnects. *Mater. Res. Symp. Proc.* 309, 199–204.
- Mahadevan, M., Bradley, R.M., 1999. Simulations and theory of electromigration-induced slit formation in unpassivated single-crystal metal lines. *Phys. Rev. B* 59 (16), 11037–11046.
- Rose, J.H., 1992. Fatal electromigration voids in narrow aluminum–copper interconnect. *Appl. Phys. Lett.* 61, 2170–2172.
- Sanchez, J.E., McKnelly, L.T., Morris, J.W., 1992. Slit morphology of electromigration-induced open circuit failures in finite line conductors. *J. Appl. Phys.* 72, 3201–3203.
- Schimschak, M., Krug, J., 1997. Surface electromigration as a moving boundary value problem. *Phys. Rev. Lett.* 78 (2), 278–281.
- Schimschak, M., Krug, J., 1998. Electromigration-induced break-up of two-dimensional voids. *Phys. Rev. Lett.* 80 (8), 1674–1677.
- Suo, Z., 1997. Motions of microscopic surfaces in materials. *Adva. Appl. Mech.* 33, 193–294.
- Suo, Z., Wang, W., Yang, M., 1994. Electromigration instability: transgranular slits in interconnects. *Appl. Phys. Lett.* 64, 1944–1946.
- Wang, W., Suo, Z., Hao, T.-H., 1996. A Simulation of electromigration-induced transgranular slits. *J. Appl. Phys.* 79 (5), 2394–2403.
- Xia, L., Bower, A.F., Suo, Z., Shih, C.F., 1997. A finite element analysis of the motion and evolution of voids due to strain and electromigration-induced surface diffusion. *J. Mech. Phys. Solids* 45 (9), 1473–1493.
- Yang, W., Suo, Z., 1996. Global view of microstructural evolution: energetics, kinetics and dynamical systems. *Acta Mech. Sinica (English Series)* 12 (2), 144–157.